Chemical Process Equipment: Selection & Design
Stanley M. Walas, Butterworth-Heinemann (1990)

Direct application of these equations in Example 6.14 is not successful, but if E_2 is taken as the reciprocal of the given expression, a plausible result is obtained.

6.9. GRANULAR AND PACKED BEDS

Flow through granular and packed beds occurs in reactors with solid catalysts, adsorbers, ion exchangers, filters, and mass transfer equipment. The particles may be more or less rounded or may be shaped into rings, saddles, or other structures that provide a desirable ratio of surface and void volume.

Natural porous media may be consolidated (solids with holes in them), or they may consist of unconsolidated, discrete particles. Passages through the beds may be characterized by the properties of porosity, permeability, tortuosity, and connectivity. The flow of underground water and the production of natural gas and crude oil, for example, are affected by these characteristics. The theory and properties of such structures is described, for instance, in the book of Dullien (*Porous Media, Fluid Transport and Pore Structure*, Academic, New York, 1979). A few examples of porosity and permeability are in Table 6.9. Permeability is the proportionality constant k in the flow equation $u = (k/\mu)\, dP/dL$.

Although consolidated porous media are of importance in chemical engineering, only unconsolidated porous media are incorporated in process equipment, so that further attention will be restricted to them.

Granular beds may consist of mixtures of particles of several sizes. In flow problems, the mean surface diameter is the appropriate mean, given in terms of the weight fraction distribution, x_i, by

$$D_p = 1/(\sum x_i/D_i). \tag{6.106}$$

When a particle is not spherical, its characteristic diameter is taken as that of a sphere with the same volume, so that

$$D_p = (6V_p/\pi)^{1/3}. \tag{6.107}$$

SINGLE PHASE FLUIDS

Extensive measurements of flow in and other properties of beds of particles of various shapes, sizes and compositions are reported by Leva et al. (1951). Differences in voidage are pronounced as Figure 6.8(c) shows.

A long-established correlation of the friction factor is that of Ergun (*Chem. Eng. Prog.* **48,** 89–94, 1952). The average deviation from his line is said to be ±20%. The friction factor is

$$f_p = \frac{g_c D_p \varepsilon^3}{u^2(1-\varepsilon)}\left(\frac{\Delta P}{L}\right) \tag{6.108}$$

$$= 150/\mathrm{Re}_p + 1.75 \tag{6.109}$$

with

$$\mathrm{Re}_p = D_p G/\mu(1-\varepsilon). \tag{6.110}$$

TABLE 6.9. Porosity and Permeability of Several Unconsolidated and Consolidated Porous Media

Media	Porosity (%)	Permeability (cm^2)
Berl saddles	68–83	1.3×10^{-3}–3.9×10^{-3}
Wire crimps	68–76	3.8×10^{-5}–1.0×10^{-4}
Black slate powder	57–66	4.9×10^{-10}–1.2×10^{-9}
Silica powder	37–49	1.3×10^{-10}–5.1×10^{-10}
Sand (loose beds)	37–50	2.0×10^{-7}–1.8×10^{-6}
Soil	43–54	2.9×10^{-9}–1.4×10^{-7}
Sandstone (oil sand)	8–38	5.0×10^{-12}–3.0×10^{-8}
Limestone, dolomite	4–10	2.0×10^{-11}–4.5×10^{-10}
Brick	12–34	4.8×10^{-11}–2.2×10^{-9}
Concrete	2–7	1.0×10^{-9}–2.3×10^{-7}
Leather	56–59	9.5×10^{-10}–1.2×10^{-9}
Cork board	—	3.3×10^{-6}–1.5×10^{-5}
Hair felt	—	8.3×10^{-6}–1.2×10^{-5}
Fiberglass	88–93	2.4×10^{-7}–5.1×10^{-7}
Cigarette filters	17–49	1.1×10^{-5}
Agar-agar	—	2.0×10^{-10}–4.4×10^{-9}

(A.E. Scheidegger, *Physics of Flow through Porous Media*, University of Toronto Press, Toronto, Canada, 1974).

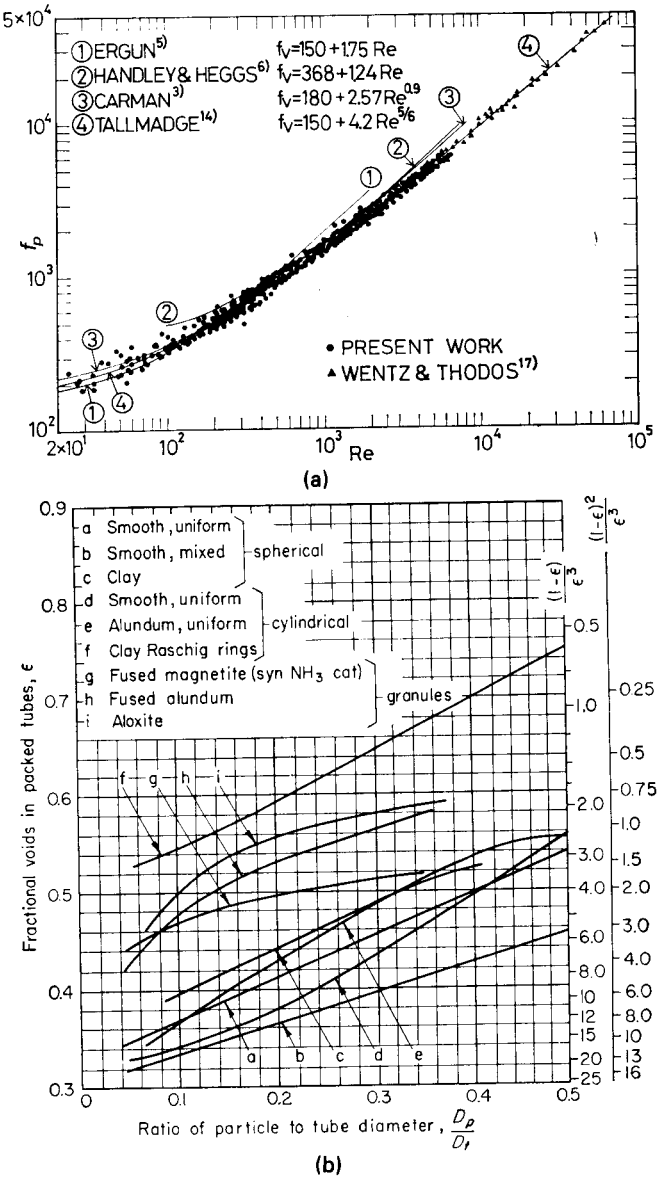

Figure 6.8. Friction factors and void fractions in flow of single phase fluids in granular beds. (a) Correlation of the friction factor, $\mathrm{Re} = D_p G/(1-\varepsilon)\mu$ and $f_p = [g_c D_p \varepsilon^3/\rho u^2(1-\varepsilon)](\Delta P/L = 150/\mathrm{Re} + 4.2/(\mathrm{Re})^{1/6}$ [*Sato et al.*, J. Chem. Eng. Jpn. **6,** *147–152 (1973)*]. (b) Void fraction in granular beds as a function of the ratio of particle and tube diameters [*Leva, Weintraub, Grummer, Pollchik, and Storch*, U.S. Bur. Mines Bull. *504 (1951)*].

The pressure gradient accordingly is given by

$$\frac{\Delta P}{L} = \frac{G^2(1-\varepsilon)}{\rho g_c D_p \varepsilon^3}\left[\frac{150(1-\varepsilon)\mu}{D_p G} + 1.75\right]. \tag{6.111}$$

For example, when $D_p = 0.005$ m, $G = 50$ kg/m^2 sec, $g_c = 1$ kgm/N sec^2, $\rho = 800$ kg/m^3, $\mu = 0.010$ N sec/m^2, and $\varepsilon = 0.4$, the gradient is $\Delta P/L = 0.31(10^5)$ Pa/m.

An improved correlation is that of Sato (1973) and Tallmadge (*AIChE J.* **16,** 1092 (1970)] shown on Figure 6.8(a). The friction factor is

$$f_p = 150/\mathrm{Re}_p + 4.2/\mathrm{Re}_p^{1/6} \tag{6.112}$$

with the definitions of Eqs. (6.108) and (6.110). A comparison of Eqs. (6.109) and (6.112) is

Re_p	5	50	500	5000
f_p (Ergun)	31.8	4.80	2.05	1.78
f_p (Sato)	33.2	5.19	1.79	1.05

In the highly turbulent range the disagreement is substantial.

TWO-PHASE FLOW

Operation of packed trickle-bed catalytic reactors is with liquid and gas flow downward together, and of packed mass transfer equipment with gas flow upward and liquid flow down.

Concurrent flow of liquid and gas can be simulated by the homogeneous model of Section 6.8.1 and Eqs. 6.109 or 6.112, but several adequate correlations of separated flows in terms of Lockhart–Martinelli parameters of pipeline flow type are available. A number of them is cited by Shah (*Gas-Liquid-Solid Reactor Design,* McGraw-Hill, New York, 1979, p. 184). The correlation of Sato (1973) is shown on Figure 6.9 and is represented by either

$$\phi = (\Delta P_{LG}/\Delta P_L)^{0.5} = 1.30 + 1.85(X)^{-0.85}, \quad 0.1 < X < 20, \tag{6.113}$$

or

$$\log_{10}\left(\frac{\Delta P_{LG}}{\Delta P_L + \Delta P_G}\right) = \frac{0.70}{[\log_{10}(X/1.2)]^2 + 1.00}, \tag{6.114}$$

where

$$X = \sqrt{(\Delta P/L)_L/(\Delta P/L)_G}. \tag{6.115}$$

The pressure gradients for the liquid and vapor phases are calculated on the assumption of their individual flows through the bed, with the correlations of Eqs. (6.108)–(6.112).

The fraction h_L of the void space occupied by liquid also is of interest. In Sato's work this is given by

$$h_L = 0.40(a_s)^{1/3}X^{0.22}, \tag{6.116}$$

where the specific surface is

$$a_s = 6(1-\varepsilon)/D_p. \tag{6.117}$$

Additional data are included in the friction correlation of Specchia and Baldi [*Chem. Eng. Sci.* **32,** 515–523 (1977)], which is represented by

$$f_{LG} = \frac{g_c D_p \varepsilon}{3\rho_G u_G^2(1-\varepsilon)}\left(\frac{\Delta P}{L}\right), \tag{6.118}$$

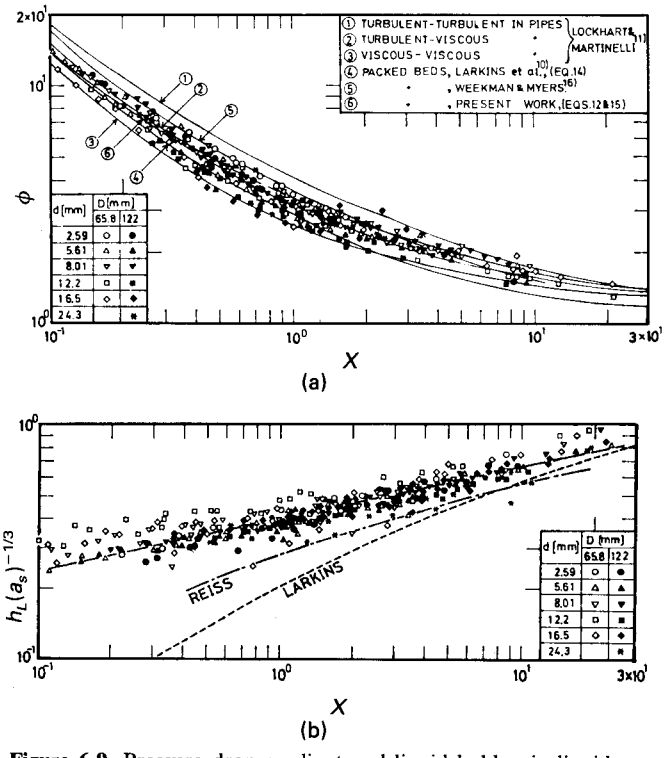

Figure 6.9. Pressure drop gradient and liquid holdup in liquid–gas concurrent flow in granular beds. [*Sato, Hirose, Takahashi, and Toda,* J. Chem. Eng. Jpn. **6,** *147–152 (1973)*]. (a) Correlation of the two phase pressure drop gradient $\Delta P/L$, $\phi = 1.30 + 1.85X^{-0.85}$. (b) Correlation of frictional holdup h_L of liquid in the bed; a_s is the specific surface, 1/mm, d is particle diameter, and D is tube diameter. $h_L = 0.4a_s^{1/3}X^{0.22}$.

$$\ln f_{LG} = 7.82 - 1.30\ln(Z/\psi^{1.1}) - 0.0573[\ln(Z/\psi^{1.1})]^2. \tag{6.119}$$

The parameters in Eq. (6.119) are

$$Z = (\mathrm{Re}_G)^{1.167}/(\mathrm{Re}_L)^{0.767}, \tag{6.120}$$

$$\psi = \frac{\sigma_w}{\sigma_L}\left[\frac{\mu_L}{\mu_w}\left(\frac{\rho_w}{\rho_L}\right)^2\right]^{1/3}. \tag{6.121}$$

Liquid holdup was correlated in this work for both nonfoaming and foaming liquids.

$$\text{Nonfoaming,} \quad h_L = 0.125(Z/\psi^{1.1})^{-0.312}(a_s D_p/\varepsilon)^{0.65}, \tag{6.122}$$

$$\text{Foaming,} \quad h_L = 0.06(Z/\psi^{1.1})^{-0.172}(a_s D_p/\varepsilon)^{0.65}. \tag{6.123}$$

The subscript w in Eq. (6.121) refers to water.

Countercurrent flow data in towers with shaped packings are represented by Figure 13.37. The pressure drop depends on the viscosity of the liquid and on the flow rates and densities of the liquid and gas, as well as on characteristics of the packing which are represented here by the packing factor F. Nominally, the packing factor is a function of the specific surface a_s and the voidage ε, as

$$F = a_s/\varepsilon^3, \tag{6.124}$$

but calculated values are lower than the experimental values shown in the table by factors of 2–5 or so. Clearly the liquid holdup reduces the effective voidage to different extents with different packings. The voidages of the packings in the table range from 70 to

Void Fraction Curve for spheres
Taken from Perry's 5th Edition
Figure 5-70

Scale x 0.003671
Scale y 0.003636

Dp/Dtube x	void y	Dp/Dtube	void
0	7.86	0.000	0.329
4.21	9.56	0.015	0.335
4.71	9.86	0.017	0.336
17.21	14.86	0.063	0.354
26.71	18.96	0.098	0.369
40.21	24.86	0.148	0.390
41.71	27.36	0.153	0.399
45.71	27.16	0.168	0.399
54.21	31.86	0.199	0.416
54.21	30.86	0.199	0.412
59.11	**32.96**	**0.217**	**0.420**
70.31	37.86	0.258	0.438
82.51	42.86	0.303	0.456
110.71	55.21	0.406	0.501
136.2	65.36	0.500	0.538

linear fit to spherical data
y = 0.4208x + 0.329

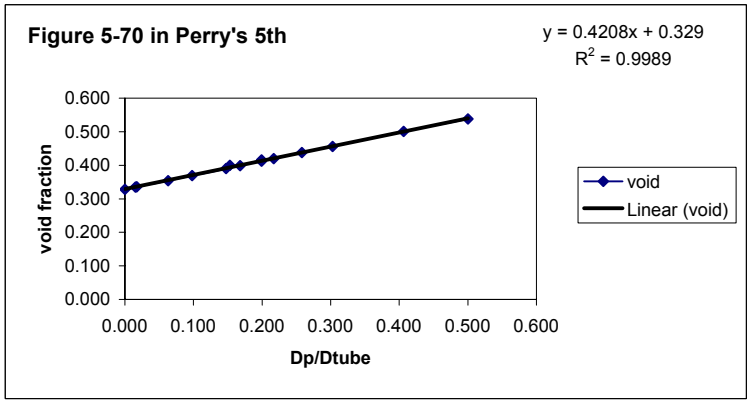

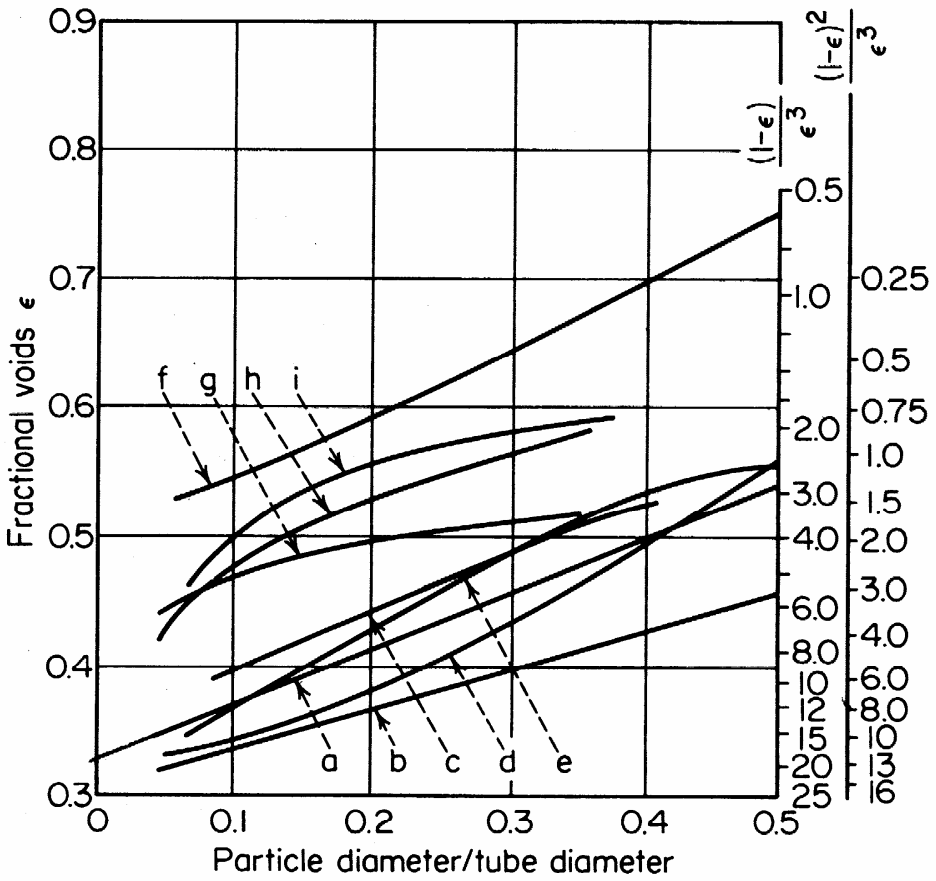

FIG. 5-70. Voidage in packed beds. Spherical: *a*, smooth, uniform; *b*, smooth, mixed; *c*, clay. Cylindrical: *d*, smooth, uniform; *e*, alundum, uniform; *f*, clay Raschig rings. Granules: *g*, fused magnetite (synthetic ammonia catalyst); *h*, fused alundum; *i*, Aloxite. (*Leva, "Fluidization," p. 54, McGraw-Hill, New York, 1959.*)